doi:10.1016/j.jmb.2008.05.010 J. Mol. Biol. (2008) 380, 820–827

JMB

Available online at www.sciencedirect.com

ScienceDirect

ELSEVIER

High-Resolution Crystal Structure of Activated Cyt2Ba Monomer from *Bacillus thuringiensis* subsp. *israelensis*

Shmuel Cohen[1,2]*, Orly Dym[3], Shira Albeck[3], Eitan Ben-Dov[1,4], Rivka Cahan[2], Michael Firer[2] and Arieh Zaritsky[1]

[1]*Department of Life Sciences, Ben-Gurion University of the Negev, P.O.B. 653, Be'er-Sheva 84105, Israel*

[2]*Department of Chemical Engineering and Biotechnology, Ariel University Center of Samaria, Ariel 40700, Israel*

[3]*The Israel Structural Proteomics Center (ISPC), Weizmann Institute of Science, Rehovot 76100, Israel*

[4]*Achva Academic College, MP Shikmim, 78900, Israel*

Received 4 March 2008; received in revised form 5 May 2008; accepted 6 May 2008
Available online 11 May 2008

Edited by I. Wilson

The Cyt family of proteins consists of δ-endotoxins expressed during sporulation of several subspecies of *Bacillus thuringiensis*. Its members possess insecticidal, hemolytic, and cytolytic activities through pore formation and attract attention due to their potential use as vehicles for targeted membrane destruction. The δ-endotoxins of subsp. *israelensis* include three Cyt species: a major Cyt1Aa and two minor proteins, Cyt2Ba and Cyt1Ca. A cleaved Cyt protein that lacks the N- and C-terminal segments forms a toxic monomer. Here, we describe the crystal structure of Cyt2Ba, cleaved at its amino and carboxy termini by bacterial endogenous protease(s). Overall, its fold resembles that of the previously described volvatoxin A2 and the nontoxic form of Cyt2Aa. The structural similarity between these three proteins may provide information regarding the mechanism(s) of membrane-perforating toxins.

Keywords: Cyt toxins; activated Cyt2Ba; insecticidal crystal proteins; membrane-active cytotoxin; X-ray crystal structure

Introduction

Bacillus thuringiensis is a species of Gram-positive, aerobic bacterium that produces endospores under certain environmental conditions.[1,2] Coincident with sporulation, it creates parasporal crystals, δ-endotoxins, composed of insecticidal crystal proteins (ICPs).[3] These entomopathogenic toxins are highly specific against larvae of Lepidoptera, Coleoptera, or Diptera[1,4] and are classified into two families: Crystal (Cry) and Cytolytic (Cyt).[5] There is no sequence or structure homology between the two families, but they share common biochemical properties. The ICPs are produced and crystallized *in vivo* as protoxins, solubilized in alkaline pH, and converted into active membrane-perforating toxins following proteolytic cleavage, removing short segments of the N and C termini.[6,7] The attachment of Cry proteins to the larval intestinal membrane is mediated through specific receptors,[8,9] whereas Cyt proteins attach nonspecifically[8] and are mediated by nonsaturated phospholipids such as phosphatidylcholine, phosphatidylethanolamine, and sphingomyelin.[10]

B. thuringiensis subsp. *israelensis* exhibits the most potent bacteria-derived mosquito larvicidal activity known so far. This stems from synergy between some of its major ICPs encoded by genes that are mapped at the 128-kb plasmid pBtoxis: four of the Cry family (Cry4Aa, Cry4Ba, Cry10Aa, and Cry11Aa) and three Cyts (Cyt1Aa, Cyt2Ba, and Cyt1Ca).[2,11]

The mosquito larvicidal activity of Cyt1Aa is lower than those of the Cry proteins, but it is highly synergistic with them.[12,13] In addition, the native protoxin

*Corresponding author. Department of Life Sciences, Ben-Gurion University of the Negev, P.O.B. 653, Be'er-Sheva 84105, Israel. E-mail address: shmulikc@ariel.ac.il.

Abbreviations used: ICP, insecticidal crystal protein; VVA2, volvatoxin A2; SE, size exclusion; RBC, red blood cell; EDTA, ethylenediaminetetraacetic acid; PDB, Protein Data Bank.

(27.2 kDa) is active *in vitro* against insect cells, erythrocytes, and mammalian cells[14] and lethal to mice following an intravenous injection.[10,14] The hemolytic and cytolytic activities of Cyt1Aa are higher than all other family members[15,16] and are enhanced by N and C termini proteolysis in the larval gut, thus forming a 22- to 25-kDa activated toxin form.[6,17,18]

Cyt1Aa (249 amino acids) shares 39% identity and 64% similarity in its amino acid sequence with Cyt2Aa (259 amino acids) from subsp. *kyushuensis*, which is also hemolytic and cytolytic following proteolytic processing in similar domains.[19] Therefore, they are likely to have a high degree of structural similarity.[19,20]

To date, the only solved crystal structure of the Cyt family is that of Cyt2Aa, which is distinguished from the Cry structure and is composed of a single α–β domain comprising two outer layers of α-helix hairpins and a β-sheet in between.[20] In the protoxin form, Cyt2Aa is a nonhemolytic[19] dimer linked by the intertwined N-terminal strands. Proteolytic processing cleaves the N- and C-terminal segments, leading to dimer dissociation and toxin activation.

The mechanism of action of Cyt toxins is still under controversy. According to one approach, the two outer layers of α-helix hairpins swing away from the β-sheet upon membrane contact, and the three last β-strands are allowed to insert into the membrane. Consequently, oligomerization with other monomers and formation of a β-barrel pore occur, resulting in a colloid osmotic lysis.[20–24] Another model suggests that the hydrophilic side of the helices interacts with residues from other monomers to form oligomer. This results in nonspecific aggregation of Cyt molecules on the surface of the lipid bilayer, leading to a detergent-like action and membrane disassembly.[10,25,26] The crystal structure of volvatoxin A2 (VVA2), a pore-forming cardiotoxin from the mushroom *Volvariella volvacea*, adopts a similar structure to that of Cyt2Aa.[27] It was suggested that the N-terminal domain of VVA2 (residues 1–127) consisting of α-helices is responsible for oligomerization, and the C-terminal domain (residues 128–199) consists of three β-strands that are inserted into the membrane.[28] These strands correspond to the strands of Cyt2Aa, which may be responsible for membrane insertion as well.

Cyt2Ba is a minor component within the complex of the crystal's proteins expressed by subsp. *israelensis*. It is composed of 263 amino acids with about of 41% and 67% identity to Cyt1Aa and Cyt2Aa, respectively.[29,30] Despite the similarities in sequences among these three Cyt proteins, no antigenic cross-reaction has been detected between them.[31] Cyt2Ba is highly homologous (more than 99% identity) to seven Cyt2Ba variants from other *B. thuringiensis* subspecies, suggesting that it is responsible for an important task within the crystal complex of this species.[29,30]

Toxicities of recombinant solubilized crystal Cyt1Aa and Cyt2Aa to mosquito larvae, as well as their hemolytic activities, are similar but higher than those of Cyt2Ba. LC_{50} values of Cyt1Aa and of Cyt2Aa against larvae of *Aedes aegypti*, *Anopheles gambiae*, and *Culex pipiens* ranged between 0.5 and 2 μg ml^{-1} and between 0.5 and 4 μg ml^{-1}, respectively, and hemolytic end-point values for undigested, endogenously digested, and fully digested Cyt1Aa were up to 3.7-fold lower than those of Cyt2Aa.[19] In another study,[15] nonsolubilized crystals of recombinant Cyt1Aa and Cyt2Ba displayed LC_{50} values of 0.4–2.7 μg ml^{-1} and 1.8–5.5 μg ml^{-1}, respectively, against larvae of *A. aegypti*, *C. pipiens*, *Culex quinquefasciatus*, and *Anopheles stephani*, whereas hemolytic end-point values of solubilized or trypsin-activated Cyt1Aa were more than 100-fold lower than those of Cyt2Ba. The reasons for the differences in activities between Cyt proteins are still unknown.

Here, we describe the crystal structure of the proteolytically cleaved active form of Cyt2Ba to 1.8 Å resolution. This is the first structure of a toxic form of a Cyt family member to be reported. The structure has a striking similarity to the protoxin form of Cyt2Aa and to fungal VVA2, suggesting that the toxic monomer of these proteins has a similar mode of activity against cell membrane.

Results and Discussion

Isolation of the Cyt2Ba monomer and its analysis and identification

Expression of *cyt2Ba* in recombinant acrystalliferous *B. thuringiensis* subsp. *israelensis* produces Cyt2Ba as easily isolatable hexagonal crystals that ranged in size from 0.4 to 0.6 μm.[32] The solubilized crystals yielded a protein that underwent partial proteolysis (Fig. 1a). The undigested Cyt2Ba appears on SDS-PAGE with a mass of 24 kDa while the endogenously digested product has a mass of 22 kDa. This mixture was purified by size exclusion (SE) chromatography yielding three peaks, including a large peak that eluted in the void volume and contained predominantly DNA (established by its 260/280 nm absorbance ratio and by lack of protein bands on SDS-PAGE). The second peak contains Cyt2Ba migrating as a dimer, which runs on SDS-PAGE as the uncleaved protein (upper band in Fig. 1a). The last peak contains Cyt2Ba migrating as a monomer on the SE column, which runs on SDS-PAGE as its degradation product (lower band in Fig. 1a). In order to obtain the fully digested product, *in vivo* Cyt2Ba crystals were solubilized in the absence of protease inhibitors at 37 °C. The fully digested Cyt2Ba (Fig. 1b) migrated on an SE column as a monomer and produced crystals for X-ray analysis, whereas the uncleaved protein (24 kDa) did not.

The activity of the cleaved purified Cyt2Ba sample was determined using hemolysis assay. Various concentrations of this fraction incubated with 0.2% of human red blood cells (RBCs) for 3 h yielded an HC_{50} value of 15.2 μg ml^{-1}. However, when the incubation was extended to 24 h, 95% hemolysis of the

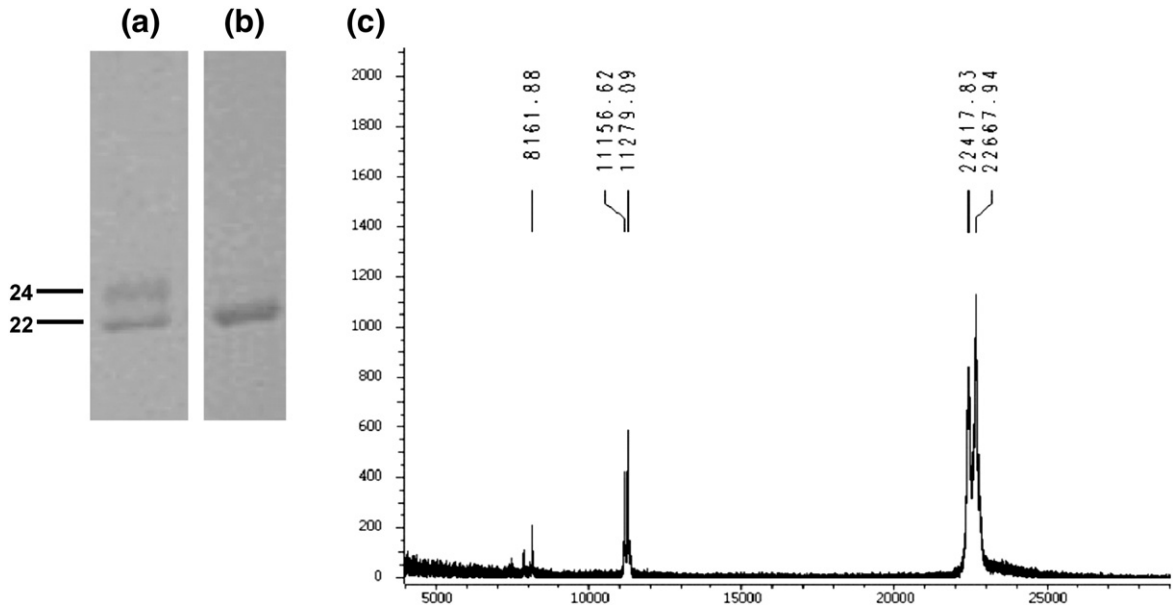

Fig. 1. Analysis of proteolytically activated Cyt2Ba. (a) SDS-PAGE analysis of Cyt2Ba extracted from crystals formed *in vivo*. This preparation contains full-length (upper band) and proteolytically digested Cyt2Ba (lower band). (b) Purified, digested Cyt2Ba, which crystallized *in vitro*. (c) MALDI-TOF mass spectrum analysis of the purified, proteolytically cleaved protein. Two fragments are identified: one with a mass of 22.4 kDa corresponding to T34–P232 (22.38 kDa) and the second fragment with a mass of 22.7 kDa corresponding to segment T34–I234 (22.6 kDa). *y*-axis, arbitrary intensity; *x*-axis, mass/charge ratio.

RBC was induced. These results are similar to those obtained with Cyt2Ba treated by endogenous proteases of subsp. *israelensis*.[32]

MALDI-TOF (matrix-assisted laser desorption/ionization time-of-flight) mass spectroscopy (Fig. 1c) of this fraction revealed two peaks, one with a mass of 22.7 kDa and the other with a mass of 22.4 kDa. The N-terminal sequence of the proteolytic fragments of solubilized *in vivo* Cyt2Ba crystals that had been treated by endogenous proteases began with residue T34.[32] Based on the masses of the two fragments, we concluded that our two fragments correspond to T34–I234 and T34–P232 (22.6 and 22.38 kDa, respectively) (marked by green arrows in Fig. 2). Interestingly, these two digested forms are homologous to the proteolytically activated fragments of Cyt2Aa digested by proteinase K (before T34 and S37 and after S228 and F237).[20]

The overall structure of monomeric Cyt2Ba

The crystal structure of the proteolytically activated, monomeric form of Cyt2Ba was solved to 1.8 Å resolution (Fig. 3). It is composed of a single domain of α/β architecture with a β-sheet surrounded by two α-helical layers representing a cytolysin fold. The sheet consists of six antiparallel β-strands (β1−β6) flanked by an α-helix layer composed of α1 and α2 on one side and by a second α-helix layer composed of α3–α5 on the other. The four longest β-strands (β2–β5) of the central β-sheet have a modified Greek-key topology. The model consists of residues T41–S228 (with 120 water molecules), while the two fragments introduced into crystallization corresponded to T34–I234 and T34–P232 (22.6 and 22.4 kDa, respectively). The lack of observed density for residues 34–40 and 229–234 in our structure suggests that these regions are disordered.

Comparison of Cyt2Ba with structurally related proteins

A striking similarity was observed between the structures of the endogenously cleaved Cyt2Ba monomer (residues T41–S228) and the corresponding region (residues D41–S228) within the inactive protoxin dimer of Cyt2Aa (rmsd of 0.59 Å). Each monomer of Cyt2Aa consists of an extra β-strand at its N terminus and α-helix at its C terminus compared to the cleaved Cyt2Ba (Fig. 4a). The dimer interface of Cyt2Aa is held together by the intertwined N-terminal strands from both monomers.[20] The cleavage of Cyt2Aa removes the N and C termini segments, thereby preventing dimer formation and, hence, releasing a monomer active toxin. Similarly, in Cyt2Ba, the proteolysis causes the removal of 34 amino acids at its N terminus and 28 or 30 residues at its C terminus, forming the crystallized toxic monomer.

Cyt2Ba shares only 16% sequence identity to VVA2 (Fig. 2). Nevertheless, they both adopt a cytolysin fold and their structure is very similar with an rmsd of 3.59 Å (Fig. 4b). VVA2 consist of 199 amino acids and possesses hemolytic and cytolytic properties.[27,28,35] The main difference between the structure of VVA2 and that of Cyt2Ba is an insertion of a β-

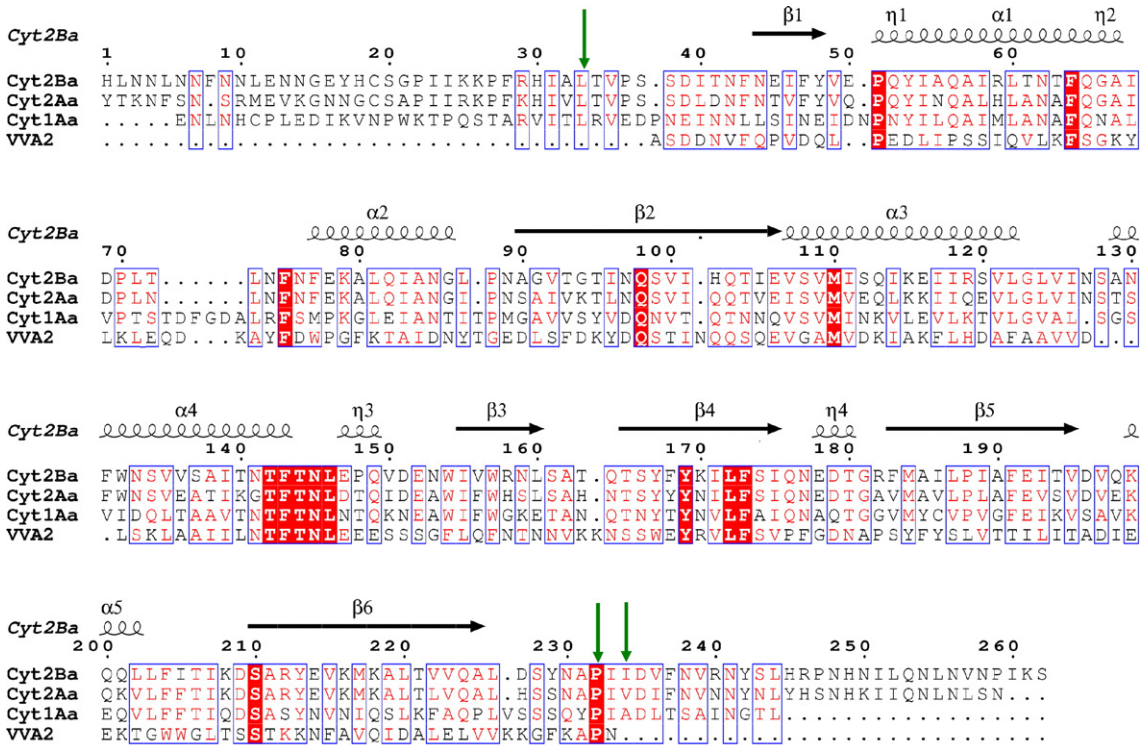

Fig. 2. Sequence alignment of Cyt2Ba, Cyt2Aa, Cyt1Aa, and VVA2. Cyt2Ba secondary structure elements are labeled above the corresponding sequence (numbering refers to the sequence of Cyt2Ba); α- and η-helices are spirals and β-strands are arrows. The residues conserved in all four proteins are in red blocks. The figure was created using ESPript.[33] Green arrows designate the proteolytic fragments T34–I234 and T34–P232.

hairpin between α1 and α2 in VVA2 (indicated by an arrow in Fig. 4b). Due to the structural resemblance between the activated forms of Cyt2Ba, Cyt2Aa, and VVA2, it seems plausible that they could have similar pore-forming mechanism(s).

VVA consists of two proteins, VVA1 and VVA2, with molecular masses of 44.8 and 22.4 kDa, respectively. While VVA2 is toxic, VVA1 does not possess any significant biological activity and is not toxic.[35] VVA1 is twice the length of VVA2, which exists only as a monomer. Interestingly, sequence alignment between VVA2 to VVA1 revealed that the VVA2 monomer is homologous to each half of VVA1 (32% identity for residues 1–189 and 36% for residues 190–393). Therefore, it is reasonable to assume that each domain of VVA1 adopts a similar fold to that observed for VVA2 and Cyt2Ba. Thus, VVA1 most likely exists as a pseudo-dimer, which may explain its lack of toxicity. The most significant outcome of this structural comparison is that the toxicity of Cyt2Ba, Cyt2Aa, and VVA2 is an inherent property of the monomer and not the result of secondary structure rearrangement upon cleavage. While the protoxins of the Cyt family form dimers, VVA2 exists solely as a monomer. Interestingly, VVA2 lacks the N- and C-terminal segments that are involved in dimer formation in the Cyt family.

Soluble VVA2 was shown to be prone to cleavage by trypsin and chemotrypsin before K127 and W132, respectively.[28] These positions are located in the region corresponding to the loop between β3 and β4 of Cyts. The aligned homologous regions in soluble Cyt1Aa, Cyt2Aa, and Cyt2Ba are protected from cleavage by these and other proteases.[6,19,32] However, when Cyt1Aa and Cyt2Aa are in a liposome-bound state, they were cleaved by trypsin and proteinase K not only at the N and C termini but also between the end of α4 and β3 (before K154 and N155 in Cyt1Aa and before G141 and I150 in Cyt2Aa), probably by changing their spatial conformation.[21] In addition, the C-terminal region of VVA2, Cyt1Aa, and Cyt2Aa starting with β4 has been shown to be resistant to proteolysis upon association to the membrane.[21,28] Therefore, it has been suggested that β4, β5, and β6 are embedded in the membrane lipid bilayer.

A comprehensive understanding of the toxic activities of these proteins may not only broaden our understanding as to the cytolytic machinery of pore-forming toxins but also help to design better membrane-active cytotoxins. Indeed, utilization of proteolytically active Cyt1Aa and Cyt2Aa in targeted drug delivery systems has recently been demonstrated: A conjugant of Cyt1Aa–insulin has been used against cells expressing high levels of insulin receptors,[36] and chemical binding or genetic fusion of active Cyt1Aa to a peptide (p87–99) of myelin basic protein (MBPp) targets Cyt1Aa to malignant B-cells expressing surface anti-MBPp antibodies.[37] In yet another study, specific toxicity against breast and ovarian cancer cells was obtained when the active

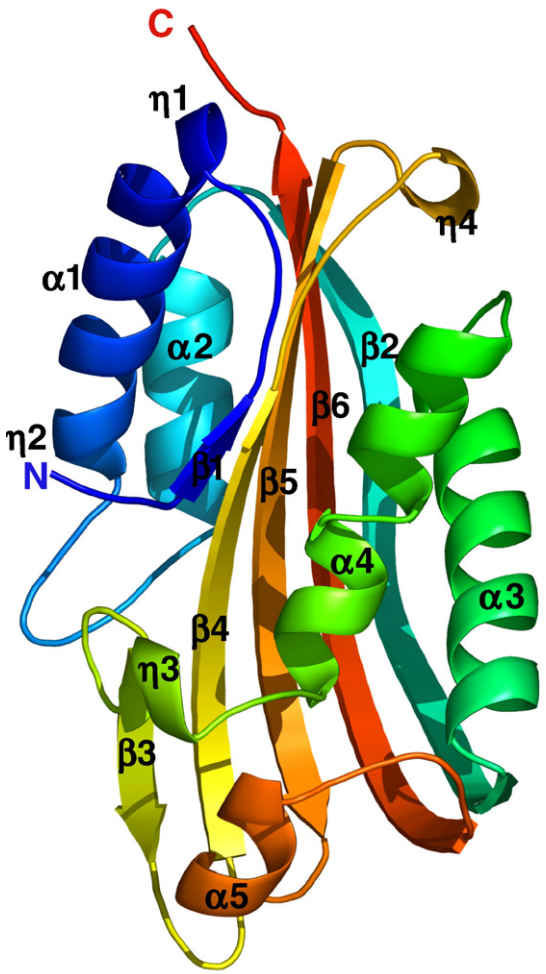

Fig. 3. Crystal structure of the Cyt2Ba monomer. Ribbon representation of the Cyt2Ba crystal structure composed of a single domain of α/β architecture with a β-sheet surrounded by two α-helical layers representing a cytolysin fold. Secondary elements and N and C termini are labeled (created with PyMOL[34]).

fragment of Cyt2Aa was genetically fused to an antibody that recognizes $p185^{HER-2}$.[38,39]

Experimental Procedures

Purification of Cyt2Ba

Strain IPS(*cyt2Ba/p20*) of acrystalliferous *B. thuringiensis* subsp. *israelensis* containing pHT*cy2B–p20*[32] and expressing *cyt2Ba* and *p20* (encoding the helper protein)[40] during sporulation was used. Cyt2Ba was assembled *in vivo* to easily isolatable hexagonal crystals, which ranged between 0.4 and 0.6 μm in size[32] after growth in CCY sporulation medium[41] for 4 days when most cells sporulated and autolyzed. The culture was centrifuged, and the sediment including crystals, spores, and debris was rinsed thrice with double-distilled water. The crystals were separated on a discontinuous sucrose gradient,[42] and the pure Cyt2Ba crystals were rinsed thrice with water and solubilized in an alkaline buffer [50 mM Na_2CO_3, pH 10.5, 5 mM PMSF, 10 mM DTT, and 10 mM ethylenediaminetetraacetic acid (EDTA)]. The supernatant was filtered and dialyzed three times against Buffer A (20 mM Tris–HCl, pH 8, 5% glycerol,

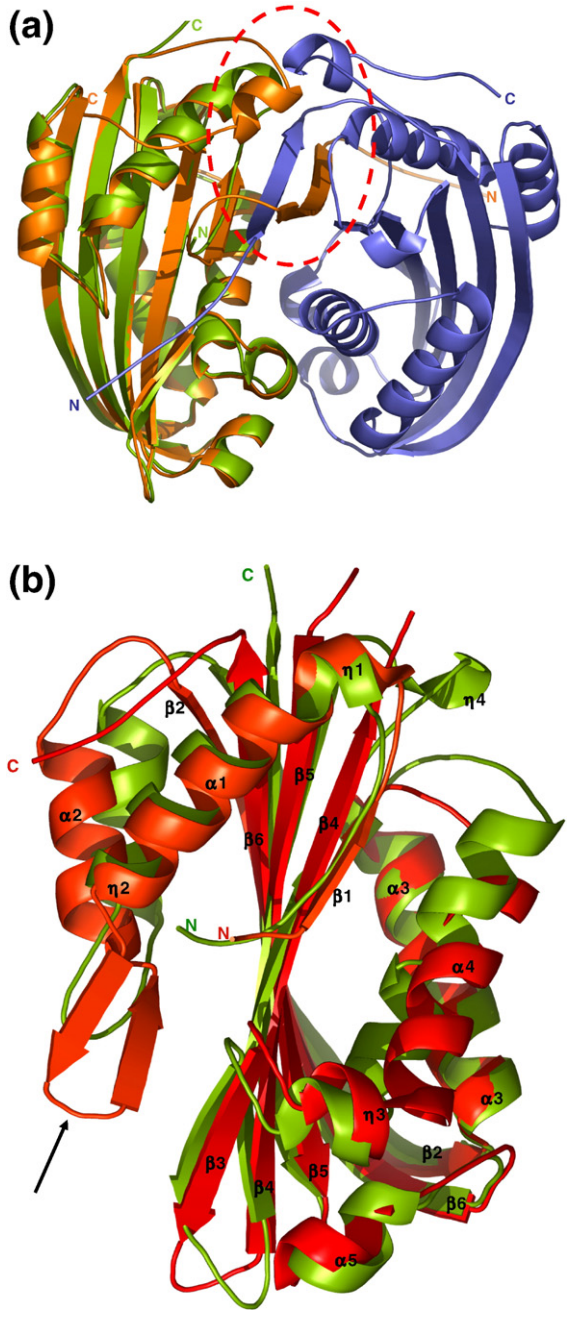

Fig. 4. Structure comparison of Cyt2Ba to Cyt2Aa and VVA2. (a) Cyt2Ba monomer (green) and Cyt2Aa dimer (monomer A, orange; monomer B, blue) (PDB accession code 1CBY). Note: the N-terminal intertwined strands and the C-terminal helices of Cyt2Aa that are both involved in dimer formation are shown in red dashed ellipsoid. Both segments do not exist in the proteolytically cleaved Cyt2Ba structure. (b) Cyt2Ba (green) and VVA2 (red). (PDB accession code 1PP0). The insertion of a β-hairpin between α1 and α2 in the VVA2 structure is shown by a black arrow. Ribbon diagrams were created by PyMOL.[34]

5 mM DTT, 1 mM EDTA, 10 mM ethanolamine, 0.1 mM PMSF, and 3 mM NaN_3).

During the preparation of soluble Cyt2Ba, there was a massive aggregation of the protoxin at neutral pH, which probably hindered its crystallization *in vitro*. Removing amino and carboxy termini of Cyt by proteolysis seemed to lower the aggregation level considerably and allowed binding to cell membrane.[6,20] For proteolyzed Cyt2Ba, the crystal sediment was incubated (1 h at 37 °C in shaker, 200 rpm) with 50 mM Na_2CO_3 buffer (pH 10.5) containing 10 mM DTT without any protease inhibitors. The supernatant was filtered, dialyzed three times against Buffer A and concentrated by placing the dialysis bag on a mat of carboxymethylcellulose (Sigma).

Proteolyzed Cyt2Ba was detected by 15% SDS-PAGE and quantified by OD_{280}. Absorbance of 1 unit is equivalent to 1.09 mg ml^{-1}.[43]

Cyt2Ba was further purified by SE chromatography (HiLoad 16/60 Superdex 75, Amersham Biosciences) with a buffer containing 20 mM Tris–HCl, pH 8, 50 mM NaCl, 5% glycerol, and 5 mM DTT. The eluted peaks were analyzed by 15% SDS-PAGE. Those containing proteolytically cleaved Cyt2Ba were pooled and concentrated by Centricon® centrifugal filter YM-10 (Millipore, Billerica, MA, USA) to a volume of 300 µl (23 mg ml^{-1} according to OD_{280}) and submitted to crystallization.

Hemolysis assay

Human RBCs were treated and analyzed as previously described.[32]

Crystallization, data collection, and refinement

Single crystals of the proteolytically cleaved Cyt2Ba (residues T34–I234) were obtained by the microbatch method under oil, using the IMPAX 1–5 robot (Douglas Instruments, East Garston, Hungerford, Berkshire, UK). The protein was crystallized in a mixture containing 1.0 M Na/K tartrate, 0.1 M Tris, pH 7.0, 0.2 M Li_2SO_4, and 10 mM EDTA sodium salt. A complete data set was collected from a single crystal on a Rigaku R-AXIS IV+ imaging plate area detector using a Rigaku RU-H3R rotating anode operated at 5 kW and Osmic multilayer X-ray focusing mirrors. The diffraction images were indexed and integrated by using the program HKL2000.[44] The integrated reflections were scaled by using the program SCALEPACK.[44] Crystals formed in space group *C*2, with cell constants $a = 83.472$ Å, $b = 43.262$ Å, $c = 55.64$ Å, and $\beta = 112.438°$, contained one monomer in the asymmetric unit cell with a V_M of 2.26 $Å^3$/Da and diffracted to 1.8 Å resolution. Structure factors' amplitudes were calculated by using TRUNCATE from the CCP4 program suite.[45] The structure was solved by molecular replacement with the program PHASER,[46] using the refined structure of the mosquito larvicidal δ-endotoxin Cyt2Aa from *B. thuringiensis* subsp. *kyushuensis* [Protein Data Bank (PDB) accession code 1CBY] as a model. All steps of atomic refinement were carried out with the program CCP4/Refmac5.[47] The model was built to σA-weighted, $2F_{obs} - F_{calc}$, and $F_{obs} - F_{calc}$ maps using the program COOT.[48] Refinement moves were accepted only when they produced a decrease in the R_{free} value. In later rounds of refinement, water molecules were built into peaks greater than 3σ in $F_{obs} - F_{calc}$ maps. The current model contains residues 44–228 and 120 water molecules. The R_{free} value is 21.6% (for the 5% of reflections not used in the refinement), and the R_{work} value is 18.7% for all data to 1.8 Å. The coordinates of Cyt2Ba have been deposited in the PDB with the accession code 2RCI. The Cyt2Ba model was evaluated with the program PROCHECK.[49] Data collection and refinement statistics are described in Table 1. The figures were created with PyMOL.[34] Sequence alignment was prepared with ESPript.[33]

Table 1. Data collection and structure refinement statistics

Data collection	
Resolution range (Å)	50.0–1.8 (1.83–1.8)
Space group	*C*2
Unit cell dimensions	
a (Å)	83.48
b (Å)	43.26
c (Å)	55.65
β (°)	112.44
Number of molecules in the asymmetric unit	1
Number of reflections measured	60,445
Number of unique reflections	16,805 (767)
R_{sym} [a]	0.075 (0.26)
Completeness (%)	97.4 (94.9)
Redundancy	3.67 (3.2)
$\langle I \rangle / \langle \sigma(I) \rangle$	16.5 (4.5)
Refinement statistics	
Resolution limits (Å)	50.0–1.8
R_{free} [b] (%)	21.6
R_{work} [b](%)	18.7
Mean *B*-factor ($Å^2$)	21.8
rmsd	
Bond lengths (Å)	0.017
Bond angles (°)	1.54
Torsion angles (°)	12.98
Ramachandran plot (%)	
Most favored	90.3
Additional allowed	9.1
Generously allowed	0.6
Disallowed regions	0.0

Values in parentheses are for the highest-resolution shells.

[a] $R_{sym} = \Sigma \; | \langle I_{hkl} \rangle - I_{hkl} | / I_{hkl} |$, where $\langle I_{hkl} \rangle$ is the average intensity over symmetry-related reflections and I_{hkl} is the observed intensity.

[b] $R = \Sigma | \; | F_o | - | F_c | \; | / \Sigma | F_o |$, where F_o denotes the observed structure factor amplitude and F_c the structure factor calculated from the model.

PDB accession code

Coordinates for the crystal structure of the Cyt2Ba-digested protein have been assigned the PDB accession code 2RCI.

Acknowledgements

We thank Prof. Joel L. Sussman for helpful discussions. We are grateful to Anna Branzburg and Yigal Michael from the Israel Structural Proteomics Center for their skilled assistance. The structure was determined at the Israel Structural Proteomics Center, supported by The Israel Ministry of Science, Culture and Sport; the Divadol Foundation; the Neuman Foundation; and the European Commission Sixth Framework Research and Technological Development Programme 'SPINE2-COMPLEXES'

Project under Contract No. 031220. Partial support was awarded by a grant (No. 2001-042) from the US–Israel Binational Science Foundation, Jerusalem, Israel (to A.Z.).

References

1. Aronson, A. (2002). Sporulation and delta-endotoxin synthesis by *Bacillus thuringiensis*. *Cell. Mol. Life Sci.* **59**, 417–425.
2. Margalith, Y. & Ben-Dov, E. (2000). Biological control by *Bacillus thuringiensis* subsp. *israelensis*. In *Insect Pest Management: Techniques for Environmental Protection* (Rechcigl, J. E. & Rechcigl, N. A., eds.), pp. 243–301, CRC press LLC, Boca Raton, FL.
3. Baum, J. A. & Malvar, T. (1995). Regulation of insecticidal crystal protein production in *Bacillus thuringiensis*. *Mol. Microbiol.* **18**, 1–12.
4. Aronson, A. I. (1993). The two faces of *Bacillus thuringiensis*: insecticidal proteins and post-exponential survival. *Mol. Microbiol.* **7**, 489–496.
5. Hofte, H. & Whiteley, H. R. (1989). Insecticidal crystal proteins of *Bacillus thuringiensis*. *Microbiol. Rev.* **53**, 242–255.
6. Al-yahyaee, S. A. S. & Ellar, D. J. (1995). Maximal toxicity of cloned CytA δ-endotoxin from *Bacillus thuringiensis* subsp. *israelensis* requires proteolytic processing from both the N- and C-termini. *Microbiology*, **141**, 3141–3148.
7. Angsuthanasombat, C., Crickmore, N. & Ellar, D. J. (1993). Effects on toxicity of eliminating a cleavage site in a predicted interhelical loop in *Bacillus thuringiensis* CryIVB delta-endotoxin. *FEMS Microbiol. Lett.* **111**, 255–261.
8. Bravo, A., Gill, S. S. & Soberón, M. (2007). Mode of action of *Bacillus thuringiensis* Cry and Cyt toxins and their potential for insect control. *Toxicon*, **49**, 423–435.
9. Pigott, C. R. & Ellar, D. J. (2007). Role of receptors in *Bacillus thuringiensis* crystal toxin activity. *Microbiol. Mol. Biol. Rev.* **71**, 255–281.
10. Thomas, W. E. & Ellar, D. J. (1983). Mechanism of action of *Bacillus thuringiensis* var. *israelensis* insecticidal delta-endotoxin. *FEBS Lett.* **154**, 362–368.
11. Berry, C., O'Neil, S., Ben-Dov, E., Jones, A. F., Murphy, L., Quail, M. A. *et al.* (2002). Complete sequence and organization of pBtoxis, the toxin-coding plasmid of *Bacillus thuringiensis* subsp. *israelensis*. *Appl. Environ. Microbiol.* **68**, 5082–5095.
12. Khasdan, V., Ben-Dov, E., Manasherob, R., Boussiba, S. & Zaritsky, A. (2001). Toxicity and synergism in transgenic *Escherichia coli* expressing four genes from *Bacillus thuringiensis* subsp. *israelensis*. *Environ. Microbiol.* **3**, 798–806.
13. Park, H. W., Bideshi, D. K. & Federici, B. A. (2003). Recombinant strain of *Bacillus thuringiensis* producing Cyt1A, Cry11B, and the *Bacillus sphaericus* binary toxin. *Appl. Environ. Microbiol.* **69**, 1331–1334.
14. Knowles, B. H., White, P. J., Nicholls, C. N. & Ellar, D. J. (1992). A broad-spectrum cytolytic toxin from *Bacillus thuringiensis* var. *kyushuensis*. *Proc. R. Soc. London, Ser. B.* **248**, 1–7.
15. Juarez-Perez, V., Guerchicoff, A., Rubinstein, C. & Delecluse, A. (2002). Characterization of Cyt2Bc toxin from *Bacillus thuringiensis* subsp. *medellin*. *Appl. Environ. Microbiol.* **68**, 1228–1231.
16. Mizuki, E., Ohba, M., Akao, T., Yamashita, S., Saitoh, H. & Park, Y. S. (1999). Unique activity associated with non-insecticidal *Bacillus thuringiensis* parasporal inclusions: *in vitro* cell-killing action on human cancer cells. *J. Appl. Microbiol.* **86**, 477–486.
17. Butko, P., Huang, F., Pusztai-Carey, M. & Surewicz, W. K. (1996). Membrane permeabilization induced by cytolytic delta-endotoxin CytA from *Bacillus thuringiensis* var. *israelensis*. *Biochemistry*, **35**, 11355–11360.
18. Du, J., Knowles, B. H., Li, J. & Ellar, D. J. (1999). Biochemical characterization of *Bacillus thuringiensis* cytolytic toxins in association with a phospholipid bilayer. *Biochem. J.* **338**, 185–193.
19. Koni, P. A. & Ellar, D. J. (1994). Biochemical characterization of *Bacillus thuringiensis* cytolytic delta-endotoxins. *Microbiology*, **140**, 1869–1880.
20. Li, J., Koni, P. A. & Ellar, D. J. (1996). Structure of the mosquitocidal delta-endotoxin CytB from *Bacillus thuringiensis* sp. *kyushuensis* and implications for membrane pore formation. *J. Mol. Biol.* **257**, 129–152.
21. Du, J., Knowles, B. H., Li, J. & Ellar, D. J. (1999). Biochemical characterization of *Bacillus thuringiensis* cytolytic toxins in association with a phospholipid bilayer. *Biochem. J.* **338**, 185–193.
22. Li, J., Derbyshire, D. J., Promdonkoy, B. & Ellar, D. J. (2001). Structural implications for the transformation of the *Bacillus thuringiensis* delta-endotoxins from water-soluble to membrane-inserted forms. *Biochem. Soc. Trans.* **29**, 571–577.
23. Promdonkoy, B. & Ellar, D. J. (2000). Membrane pore architecture of a cytolytic toxin from *Bacillus thuringiensis*. *Biochem. J.* **350**, 275–282.
24. Promdonkoy, B. & Ellar, D. J. (2005). Structure–function relationships of a membrane pore forming toxin revealed by reversion mutagenesis. *Mol. Membr. Biol.* **22**, 327–337.
25. Butko, P. (2003). Cytolytic toxin Cyt1A and its mechanism of membrane damage: data and hypotheses. *Appl. Environ. Microbiol.* **69**, 2415–2422.
26. Manceva, S. D., Pusztai-Carey, M., Russo, P. S. & Butko, P. (2005). A detergent-like mechanism of action of the cytolytic toxin Cyt1A from *Bacillus thuringiensis* var. *israelensis*. *Biochemistry*, **44**, 589–597.
27. Lin, S. C., Lo, Y. C., Lin, J. Y. & Liaw, Y. C. (2004). Crystal structures and electron micrographs of fungal volvatoxin A2. *J. Mol. Biol.* **343**, 477–491.
28. Weng, Y. P., Lin, Y. P., Hsu, C. I. & Lin, J. Y. (2004). Functional domains of a pore-forming cardiotoxic protein, volvatoxin A2. *J. Biol. Chem.* **279**, 6805–6814.
29. Guerchicoff, A., Delecluse, A. & Rubinstein, C. P. (2001). The *Bacillus thuringiensis* cyt genes for hemolytic endotoxins constitute a gene family. *Appl. Environ. Microbiol.* **67**, 1090–1096.
30. Guerchicoff, A., Ugalde, R. A. & Rubinstein, C. P. (1997). Identification and characterization of a previously undescribed cyt gene in *Bacillus thuringiensis* subsp. *israelensis*. *Appl. Environ. Microbiol.* **63**, 2716–2721.
31. Held, G. A., Kawanishi, C. Y. & Huang, Y. S. (1990). Characterization of the parasporal inclusion of *Bacillus thuringiensis* subsp. *kyushuensis*. *J. Bacteriol.* **172**, 481–483.
32. Nisnevitch, M., Cohen, S., Ben-Dov, E., Zaritsky, A., Sofer, Y. & Cahan, R. (2006). Cyt2Ba of *Bacillus thuringiensis israelensis*: activation by putative endogenous protease. *Biochem. Biophys. Res. Commun.* **344**, 99–105.
33. Gouet, P., Courcelle, E., Stuart, D. I. & Metoz, F. (1999). ESPript: analysis of multiple sequence alignments in PostScript. *Bioinformatics*, **15**, 305–308.
34. DeLano, W. L. (2002). The PyMOL molecular graphics system. *DeLano Scientific, San Carlos, CA, USA.* http://www.pymol.org.

35. Lin, J. Y., Jeng, T. W., Chen, C. C., Shi, G. Y. & Tung, T. C. (1973). Isolation of a new cardiotoxic protein from the edible mushroom, *Volvariella volvacea*. *Nature*, **246**, 524–525.
36. Al-yahyaee, S. A. & Ellar, D. J. (1996). Cell targeting of a pore-forming toxin, CytA delta-endotoxin from *Bacillus thuringiensis* subspecies *israelensis*, by conjugating CytA with anti-Thy 1 monoclonal antibodies and insulin. *Bioconjugate Chem.* **7**, 451–460.
37. Cohen, S., Cahan, R., Ben-Dov, E., Nisnevitch, M., Zaritsky, A. & Firer, M. A. (2007). Specific targeting to murine myeloma cells of Cyt1Aa toxin from *Bacillus thuringiensis* subspecies *israelensis*. *J. Biol. Chem.* **282**, 28301–28308.
38. Gurkan, C. & Ellar, D. J. (2003). Expression in *Pichia pastoris* and purification of a membrane-acting immunotoxin based on a synthetic gene coding for the *Bacillus thuringiensis* Cyt2Aa1 toxin. *Protein Expr. Purif.* **29**, 103–116.
39. Gurkan, C. & Ellar, D. J. (2003). Expression of the *Bacillus thuringiensis* Cyt2Aa1 toxin in *Pichia pastoris* using a synthetic gene construct. *Biotechnol. Appl. Biochem.* **38**, 25–33.
40. Shao, Z. & Yu, Z. (2004). Enhanced expression of insecticidal crystal proteins in wild *Bacillus thuringiensis* strains by a heterogeneous protein P20. *Curr. Microbiol.* **48**, 321–326.
41. Stewart, G. S., Johnstone, K., Hagelberg, E. & Ellar, D. J. (1981). Commitment of bacterial spores to germinate. A measure of the trigger reaction. *Biochem. J.* **198**, 101–106.
42. Debro, L., Fitz-James, P. C. & Aronson, A. (1986). Two different parasporal inclusions are produced by *Bacillus thuringiensis* subsp. *finitimus*. *J. Bacteriol.* **165**, 258–268.
43. Cantor, C. R. & Schimmel, P. R. (1980). In *Biophysical Chemistry, Part II: Techniques for the Study of Biological Structure and Function*. pp. 380–381, W. H. Freeman and Co., San Francisco, CA.
44. Otwinowski, Z. & Minor, W. (1997). Processing of X-ray Diffraction Data Collected in Oscillation Mode. In *Methods in Enzymology* (Carter, J. C. W. & Sweet, R. M., eds.), Vol. 276, pp. 307–326, Academic Press, New York.
45. French, G. S. & Wilson, K. S. (1978). On the treatment of negative intensity observations. *Acta Crystallogr., Sect. A: Cryst. Phys., Diffr., Theor. Gen. Crystallogr.* **34**, 517–525.
46. McCoy, A. J. (2007). Solving structures of protein complexes by molecular replacement with Phaser. *Acta Crystallogr., Sect. D: Biol. Crystallogr.* **63**, 32–41.
47. Murshudov, G. N., Vagin, A. A. & Dodson, E. J. (1997). Refinement of macromolecular structures by the maximum-likelihood method. *Acta Crystallogr., Sect. D: Biol. Crystallogr.* **53**, 240–255.
48. Emsley, P. & Cowtan, K. (2004). Coot: model-building tools for molecular graphics. *Acta Crystallogr., Sect. D: Biol. Crystallogr.* **60**, 2126–2132.
49. Laskowski, R. A., MacArthur, M. W., Moss, D. S. & Thornton, J. M. (1993). PROCHECK: a program to check the stereochemical quality of protein structures. *J. Appl. Crystallogr.* **26**, 283–291.